



Upheaval buckling of reeled flowlines



Unrestricted

SR.12.12579

Upheaval buckling of reeled flowlines
by
R. Peek (GSNL-PTE/EPFA)
G. Stewart (Lloyd's Register of Shipping, Aberdeen)

This document is unrestricted.

Copyright Shell Global Solutions International, B.V. 2012.

Shell Global Solutions International B.V., Rijswijk

Further electronic copies can be obtained from the Global Information Centre.

Executive summary

Preface

This report is a slightly revised version of a paper presented at the OMAE 1998 Conference in Lisbon. The paper had not been included in the conference proceedings (since it had not been ready on time), but hardcopies were distributed at the time of the presentation in Lisbon. Since the findings and conclusions of this paper remain valid, and largely not been superseded, this report serves as an accessible record of the paper.

Abstract

In the North Sea flowlines are often buried to protect them from fishing gear. In such constrained pipes, significant axial compressive forces develop due to thermal and pressure loads, and these can lead to upheaval buckling. Indeed there have been a number of upheaval buckles in recent years, and this has prompted some further study into this phenomenon to determine whether existing design procedures are adequate. This paper addresses primarily the influence of reeling of the pipeline on upheaval buckling, although other sources that may affect the buckling response, such as lack of infill under the pipe, are also considered. Reeling affects the properties of the pipe in four potentially significant ways: (i) The plastic deformations due to reeling will leave residual stresses locked in the pipe. As a result, upon subsequent loading due to temperature and pressure, yielding will occur at a lower level of load. (ii) Prior plastic deformation due to reeling essentially reduces the yield stress for subsequent loading (Baushinger effect). Consequently, a reeled pipe will start yielding at lower bending moment and/or axial force. (iii) Some reduction in the flexural resistance also occurs due to ovalisation of the cross section. (iv) The pipe may not have been properly straightened after reeling, due to variability in pipe properties, or some other reason.

To address how these effects of reeling influence the pipe response, the moment-curvature relationship is firstly examined. Then the entire process of reeling followed by laying of the pipe, covering it, and applying the temperature and pressure loads is simulated by the finite element method, using a constitutive relation for the steel that properly models the Baushinger effect. The effect of improper straightening is also considered. The results indicate that although reeling causes a softening effect on the moment curvature relationship, this is largely compensated for by a corresponding softening of the axial force-deformation characteristics of the pipe, by which the driving forces for upheaval buckling are reduced. Thus in the cases considered, reeling does not appear to significantly affect the upheaval buckling temperature. Infill of any gaps under the pipe is found have more influence, as without such infill large local curvatures may develop which significantly reduce the buckling temperature. The finite element results also show that the maximum uplift resistance force in the soil is developed only over a relatively short length to each side of the crest of the imperfection. As a result analytical formulae based on the assumption that the maximum hold down force is developed over a longer length of pipe yield unconservative predictions. On the other hand simple formulae presented here, based on locating inflection points on the pipe profile give generally good agreement with the finite element results computed in this paper.

Table of contents

Executive summary	II
1. Introduction	1
2. Loading History due to Reeling	2
3. Finite Element Formulation for Upheaval Buckling	3
4. Example Problem	5
5. Loading History	7
6. Results	9
7. Accuracy of Simplified Methods	10
7.1. Prop without infill	10
7.2. Prop with infill before covering	11
7.3. Updated Design Curve	12
8. Conclusions	13
9. Acknowledgements	14
References	15
Bibliographic information	22
Report distribution	23

List of figures

Figure 1:	Distribution of axial residual stresses in a pipe reeled to a bending strain of 10 times the yield strain, based on beam theory for elastic-perfectly plastic material behaviour.	16
Figure 2:	Typical cyclic stress-strain relation from a seamless grade X65 carbon steel pipe. Results are from a coupon test involving loading in the axial direction of the pipe at room temperature. Parameters for Dafalias model [1] fit shown inside figure. (These are the material parameters used for the analyses).	16
Figure 3:	Moment-curvature relationship during reeling for a grade X65 carbon steel pipe with stress-strain behaviour shown in Figure 2 and an outer diameter to thickness ratio of $D/t=20$. [Beam model results do not include ovalisation and are independent of D/t .]	17
Figure 4:	Moment-curvature relationship for an as-laid grade X65 carbon steel pipe with stress-strain behaviour shown in Figure 2 and $D/t=20$. [After reeling the pipe is kept straight while being subjected to internal pressure generating a hoop stress of 72% of the specified minimum yield stress (SMYS), and an axial load equivalent to that which would develop in an axially constrained elastic pipe under internal pressure plus a temperature rise of 1000C. The bending deformations are then applied under constant pressure and axial load].	17
Figure 5:	Comparison of upheaval buckling temperatures for reeled pipes (continuous lines) to those for virgin pipe (dotted lines) under various conditions. [ID=200mm, $D/t=15$, Prop Height = 0.3m, grade X65 carbon steel as in Figure 2, No residual curvatures].	18
Figure 6:	Effect of residual curvature on the upheaval buckling temperature of reeled pipe. The residual curvature corresponds to a bending strain of 0.05% (convex upwards), and is present over a length of 5m to each side of the prop imperfection. [ID=200mm, $OD/t=15$, Prop Height=0.3m, X65 carbon steel as in Figure 2, Reeled Pipe for all cases].	18
Figure 7:	Comparison of incipient uplift temperatures for reeled pipes (continuous line) to those for virgin pipe (dotted lines) under various conditions. The incipient uplift temperature is defined as the temperature at which the pipe first loses contact from the prop foundation imperfection. [ID=200mm, $OD/t=15$, Prop Height = 0.3m, X65 carbon steel as in Figure 2, No residual curvatures].	19
Figure 8:	Effect of residual curvature on the incipient uplift temperature of reeled pipe. The residual curvature corresponds to a bending strain of 0.05% (convex upwards), and is present over a length of 5m to each side of the prop imperfection. [ID=200mm, $OD/t=15$, Prop Height=0.3m, X65 carbon steel as in Figure 2, Reeled Pipe for all cases].	19
Figure 9:	Effect of reeling on effective net axial force developed in a fully constrained line	20
Figure 10:	Comparison of upheaval buckling temperatures for case of no infill. [ID=200mm, $OD/t=15$, Prop Height=0.3, X65 Carbon steel as in Figure 2].	20

- Figure 11: Comparison of upheaval buckling temperatures for case when any gaps under the pipe are filled in with soil before covering. [ID=200mm, OD/t=15, Prop Height=0.3, X65 Carbon steel as in Figure 2]. 21
- Figure 12: Updated design curve for the dimensionless required uplift resistance Φ_q (Eq. 4) as a function of the dimensionless wavelength of the imperfection Φ_L (Eq. 5b), and comparison with results from finite element analyses. 21

1. Introduction

Reeling has proven to be a cost effective installation method for flowlines. Essentially the pipe string is fabricated on-shore, and then spooled onto a large reel on board a vessel. As a result, no offshore welding is required. To install the pipe offshore it is simply unspooled, straightened and laid. In the process the pipe is subjected to bending strains around 10 times the yield strain. This can affect the subsequent behaviour of the pipe in the following ways:

- (i) Typical residual stresses in the as-laid line caused by reeling to 10 times the yield strain in an elastic perfectly plastic pipe are shown in Figure 1. As a result, if the pipe on the sea-bed is bent in the reeling direction, it will start yielding at 74% of the yield moment of a virgin pipe. Under axial loads it will start yielding at 22% of the axial yield load of a virgin pipe. This clearly has consequences for upheaval buckling where one depends to some extent on the bending resistance of the pipe.
- (ii) Real pipe materials are not elastic-perfectly plastic. A typical stress-strain relation is shown in Figure 2. It indicates that although upon first loading the material behaviour is indeed well approximated by the elastic-perfectly plastic idealisation, upon reversal of the load the nonlinear material behaviour begins at much lower stresses. This is the so-called Baushinger effect. Indeed for the test of Figure 2, nonlinearity is already apparent during unloading, before reverse loading starts. (The measured tangent modulus at zero stress is about 70% of the initial value). Clearly this will have an effect, since both the flexural stiffness as well as flexural strength of the pipe play a role in upheaval buckling.
- (iii) Plastic bending and straightening of the pipe will typically lead to some ovalisation of the cross section. Typically, however, this ovalisation is not more than 2%. This will lead to about 4% reduction in the elastic flexural stiffness, and 2% reduction in the fully plastic bending capacity. Thus the effect of ovality appears to be small compared to the above two effects.
- (iv) After reeling the pipe should be straight when it is not subjected to any bending moment. Any out-of-straightness (OOS) that remains after reeling at zero bending moment may be referred to as inherent pipe OOS. This is more detrimental than OOS that arises due to an uneven seabed profile. Even if the laybarge is equipped with a perfectly rigid straightener by which true curvature control on the pipe can be achieved, inherent pipe OOS can still arise due to variations in the pipe properties. For instance a change in the yield stress $\Delta\sigma_y$ will lead to inherent pipe OOS corresponding to a bending strain of about $\Delta\sigma_y / E$, where E is Young's Modulus. Larger pipe OOS will result from changes in yield stress if curvature control is not achieved in the straightener. On this basis an inherent pipe OOS corresponding to a bending strain of 0.05% (or 0.05% inherent pipe OOS, for short) will be taken as a reference value.

To study the above effects, the influence on the moment-curvature diagram is firstly considered. Then the entire reeling process followed by laying, backfilling, and applying the pressure and temperature loads is simulated.

As an example, a grade X65 carbon steel pipe is considered, with an inner diameter of 200mm, and an outer diameter to thickness ratio of $D/t=15$. To represent the stress-strain behaviour the Dafalias Model [1] with the Mhroz direction of strain hardening is used. Figure 2 shows how the results from this model match the uniaxial coupon test results. Unless otherwise noted all results given are for this reference case.

2. Loading History due to Reeling

As a typical value, a 2% bending strain on the reel is assumed. Also for simplicity the same bending strain is assumed for the aligner. The curvature history due to reeling thus involves (i) bending to 2% strain, (ii) straightening to 0% strain, (iii) rebending over the aligner to 2% strain, (iv) passing the pipe through the straightener which imposes a -0.322% bending strain¹ (i.e. reverse bending), such that the bending strain is zero when (v) the straightening moment is released. The axial forces are typically small during this process and are therefore neglected.

Two types of model are used to simulate reeling. The first is a slice model based on a two-dimensional discretisation of the cross section of the pipe using generalised plane strain elements. This is essentially an exact model for a pipe under uniform bending, involving no approximations such as those of a beam or shell theory. It also includes the effect of ovalisation of the cross section, which is determined as part of the slice model analysis. A much simpler analysis is performed using a beam model. This is based on conventional beam bending theory, and does not account for ovalisation. For this model, the stresses are calculated at 20 evenly spaced integration points around the cross section of the pipe, and integrated to obtain the bending moment and axial force at the cross section. The effect of internal pressure is also included in the beam model, by including a hoop stress of $p(D-t)/(2t)$ in the stress calculation at every integration point, where p is the net internal pressure, D is the outer diameter, and t the wall thickness.

The moment curvature history during reeling is shown in Figure 3 for both the slice and the beam models. Clearly the beam model provides a good approximation, confirming that the effect of ovality is small.

Also of interest is the moment-curvature relation in the presence of the pressure and axial loads that will be present in the in-service condition. Figure 4 shows the moment curvature relations for a pipe pressurised to 50% of the yield pressure², and with an axial load equivalent to that which a fully constrained pipe would experience if it remained elastic under the combined action of the internal pressure and a temperature rise of 100°C. The bending response for both the virgin pipe, as well as for pipe that has been subjected to the prior reeling deformations are plotted. This illustrates the effect of reeling: not only does it produce a significant reduction in flexural resistance, but also a nonzero moment is found at zero curvature for the reeled pipe. This means that under applied pressure and axial load a reeled pipe will develop a bending moment if it is kept straight.

Conversely, this implies that a reeled pipe will bend under internal pressure and axial load only with no bending moment applied.

In all cases it is found that the beam model provides a good approximation to the more complete slice model. Therefore the beam model is used in simulating upheaval buckling as it has the advantage of much greater simplicity. This is important as the simulation of upheaval buckling requires simultaneous consideration of quite a number of cross sections of the pipe along its length that are subjected to different bending and axial load histories.

¹ These quoted bending strains are nominal bending strains defined as the curvature of the pipe times one half the outer diameter. Positive bending strains imply the pipe is convex on the upper side.

² Here the yield pressure is taken as $p = 2 \text{ SMYS } t / D$, where SMYS is the specified minimum yield strength of 65ksi (448 MPa).

3. Finite Element Formulation for Upheaval Buckling

The formulation used is based on moderate deflection beam theory in which the effect of the hoop stress due to internal pressure on the axial stress-strain relationship is included. Thus the axial strain at any point on the cross section of the pipe is taken to be

$$\varepsilon = u' + w'/2 - w''z$$

where u and w are the axial and vertical displacements, respectively, z is the change in elevation from the centre of the pipe to the point under consideration, and a prime denotes differentiation with respect to the axial coordinate.

The discretisation is based on linear interpolation of both the displacements and rotations between nodal points, and integration of the virtual work at a single cross section in the middle of each element, using 20 integration points around the circumference to integrate the virtual work associated with axial stresses. Shear deformations are included in this formulation, but not expected to be important. Therefore, for the sake of simplicity, the shear resistance is based on the assumption of elastic behaviour and uncoupled from axial and bending effects on the cross section. For the integration across the wall thickness a single point at the midsurface is used. This amounts essentially to a thin-walled shell approximation for the pipe. The hoop stress is also based on this thin walled shell approximation, using the diameter to the midsurface.

The convergence of this finite element formulation as the number of elements increased was found to be essentially as good as for the more complicated cubic hermitian elements, which can become quite ill conditioned for short elements because shear flexibility is not included in the cubic hermitian formulation. For a number of test cases involving both elastic, and elastic-perfectly plastic behaviour of the pipe, it was found that the formulation lead to upheaval buckling temperatures (at loss of stability) within 1°C of those from an existing code [2], [3].

To account for the Baushinger effect, the material model of Dafalias [1] is used. This model is based on a yield surface that can translate in stress space (as for kinematic hardening), and a bounding surface, that is used to define the incremental moduli during plastic loading. This Dafalias material model has been used quite extensively by Kyriakides [4], [5] in comparisons with experimental data and has proven capable of matching the experimental data under a variety of cyclic loading conditions. It must be borne in mind, however, that over time the material may recover from the Baushinger effect, especially at higher temperatures, a phenomenon that is thought to be associated with diffusion of certain elements (such as nitrogen) into dislocation sites, and thereby inhibiting further propagation of the dislocation.

Reeling is simulated by imposing initial bending strains while keeping the pipe straight, but axially unrestrained. That way the history of axial stresses and strains during reeling is reproduced, without having to model the contact problem of the pipe coming onto and off the reel, aligner and straightener.

The soil resistance is modelled in a standard manner [2], [3] by using springs that remain linearly elastic until a mobilisation displacement is reached, beyond which the uplift resistance remains essentially constant (except for small adjustments to allow for changes in the cover height based on the assumption that the elevation of the top of the cover does not change). For the cohesionless cover model used here the weight of the soil directly above the pipe exerts an essentially constant downward force, of $\gamma H D$, where γ is the effective weight of the soil, D is the outer diameter of the pipe including any coatings, and H is the current cover height measured from the top of the pipe to the top of the cover. Additional hold-down force is mobilised as a linear function of the upward displacement increment after backfilling, up to maximum amount of $\gamma H (D + f H)$, where f is the friction factor for uplift resistance provided by the cover.

Details of the formulation of the cover and foundation springs are given in [2], [3]. Here a capability was also included to fill any gaps under the pipe in with soil at any specified time. The foundation with infill is taken to have the same stiffness as without infill.

4. Example Problem

As an example, a carbon steel pipe with material properties shown in Figure 2 is considered, which is laid onto a flat foundation with a “sharp” 0.3m high prop imperfection. The internal pressure is taken to be 29.87 MPa, which is 50% of the yield pressure as calculated based on the outer diameter of the pipe using the specified minimum yield stress of X65 carbon steel. The following parameters are fixed:

Inner Diameter	200mm
Outer Diameter to Wall Thickness Ratio (D/t)	15
Coating Thickness	37mm
Coating Density	757 kg/m ³
Steel Density	7790 kg/m ³
Pipe Contents Density	1000 kg/m ³
Seawater Density	1025 kg/m ³
Young's Modulus	210 GPa
Poisson's Ratio	0.3
Coefficient of Thermal Expansion	0.117% per 100°C
Lay Tension	None.
Height of Prop Imperfection	0.3m
Cohesionless Cover Submerged Weight	9.5 kN/m ³
Friction Factor f for cover uplift resistance [2,3]	0.5
Mobilisation displacement for uplift resistance	15mm
Friction factor for axial soil force (cover & foundation)	0.5
Mobilisation displacement for axial friction force	5mm
Foundation Stiffness (for downward forces)	25 MN/m ²

The parameters varied to investigate their effect are described below:

- 1) Pipe imperfections in the form of residual curvature are considered as follows: (a) no residual curvature and (b) a convex upward residual curvature corresponding to 0.05% bending strain in that part of the pipe within 5m of the prop imperfection, and no residual curvatures elsewhere.
- 2) Both (a) virgin pipe and (b) reeled pipe are considered. The reeled pipe has been reeled to 2% strain, straightened to zero bending strain, re-bent to 2% strain on the aligner, and straightened by reverse bending to -0.322% strain. It is assumed that the pipe is spooled onto the top of the reel, so that the bending deformations during spooling involve tension at the 12 o'clock position of the pipe cross section. Furthermore it is assumed that there is no twisting of the pipe, so that a point on the pipe that is in the 12 o'clock position during spooling will also be in the 12 o'clock position when the pipe is lying on the seafloor.
- 3) In all cases the foundation consists of a 0.3m-high sharp prop on an otherwise flat seabed. However three different assumptions are considered regarding the gaps under the pipe that exists to each side of the prop: (a) the gaps under the pipe are filled in by soil before the pipe

is covered, (b) the gaps remain during covering of the pipe³, but are then filled in before application of temperature and pressure loads, and (c) the gaps are never filled in. In all cases the foundation with fill material is assumed to have the same stiffness of 25 MN/m² as the original foundation.

- 4) Cover heights ranging from 0.75m to 2.5m are considered. The cover heights quoted are from the top of the pipe to the top of the cover over those portions of the pipe that are not affected by the foundation prop (the cover height at the prop is less by about 0.3m).

The finite element discretisation is based on 0.5m-long 2-noded elements from the prop ($x=0$) to a distance of $x=50$ m from the prop. The next 1km of the pipeline (from $x=50$ m to $x=1050$ m) does not upheave, but it does provide some feed in by axial displacements of the pipe partially restrained by axial soil friction. For this feed-in length, 20 elements with lengths varying uniformly from 2.25m at $x=50$ m to 92.75m at $x=1050$ m are used. The rotations throughout this feed-in length of the pipe are set to zero, and, to further reduce the number of degrees of freedom, the vertical displacements are assumed to be constant throughout all feed-in elements⁴ so that only one vertical displacement degree of freedom needs to be used for this 1km-long portion of the pipeline. The end of this feed-in length (at $x=1050$ m) is assumed to be unrestrained in the axial direction. It is far enough away to have no influence on upheaval at the prop imperfection ($x=0$)⁵.

³ As in the UPBUCK2 formulation, the downward load due to covering of the pipe is taken to be the submerged weight of the column of soil of width equal to the outer diameter of the pipe (including coating) above the pipe.

⁴ This assumption is justified here because the amount of cover and the foundation conditions are constant over the whole feed-in length. If this were not so, the assumption of constant vertical displacements along the feed-in portion of the line should not be used.

⁵ Indeed analyses with different levels of force applied at the end, ranging from zero to the fully restrained force that develops under elastic conditions showed no appreciable difference in upheaval buckling temperature.

5. Loading History

The loading is specified as a function of a load parameter denoted here by t . This parameter may be thought of as a time parameter. Of course, since the model used here does not involve any viscosity, inertia, or other time dependent effects, any time parameter could be used to describe the various events in the loading history. These events are as follows:

- 1) Initially, at $t=0$, the pipe is taken to be straight, and at an elevation of $y=0.3\text{m}$, so that it just touches the highest point on the foundation. There are no loads and the pipe is held in place by artificial springs, which are to be subsequently removed.
- 2) The curvature history due to reeling and straightening of the pipe is simulated by applying a time-varying initial curvature. The boundary conditions are such that the transverse displacements and nodal rotations remain zero throughout this process, as does the axial force. Nevertheless the axial stresses and mechanical strains are those of the reeling and straightening process. This process is complete at time $t=4.2$, and it includes spooling (till $t=1$), unspooling (till $t=2$), re-bending over the aligner (till $t=3$), straightening (till $t=4$), and removing the straightening curvature (till $t=4.2$). Small steps involving an increment in the load parameter t of 0.002 per step are used throughout to ensure accurate results despite the explicit forward difference approach used for the integration of the Dafalias constitutive equations [1].
- 3) Laying of the pipe is simulated by gradually removing the artificial springs that initially support it. This is done by reducing their stiffness gradually to zero⁶. At the same time the submerged weight of the pipe is applied, which here is taken be the flooded weight. During this process the axial friction coefficient for the foundation is set to zero, to avoid axial forces being generated in the pipe. Laying tension may then be applied at the end, although in the analyses presented here, zero laying force is used. Once the laying is complete, the axial friction of the foundation is activated, allowing axial forces to be generated during the next step. Laying occurs between $t=4.2$ and $t=4.7$.
- 4) If there is to be any residual curvature in the pipe, this is introduced at the beginning of the laying process (between $t=4.2$ and $t=4.4$) by introducing an initial curvature into the appropriate pipe elements (i.e. first 10 pipe elements starting from the prop). The initial curvature in this case involves the pipe becoming convex on the upper side within 5m from the prop imperfection.
- 5) Covering of the pipe involves applying an additional vertical load due to the weight of cover resting directly above the pipe. This occurs between $t=4.7$ and $t=4.8$. Upon completion of covering, the profile of the pipe is stored, and it is the subsequent changes in vertical displacement from that time that determine how much cover force is mobilised [2], [3]. Also, the cover component of the axial friction force can begin to be mobilised at this time. Filling of any gaps under the pipe is done either at the beginning of the covering operation (at $t=4.7$), or at the end ($t=4.8$). To achieve this, the coordinates of the foundation profile are modified, so that they match those of the pipe at the appropriate time and locations⁷.
- 6) Pressurisation of the pipe takes place between $t=4.8$ and $t=5.0$.
- 7) Finally the thermal strains are applied. In order that converged solutions can be obtained up to and beyond the point where stability is lost an arclength method generally attributed to Riks [6], [7] is used. This means that instead of specifying an increment in the load parameter

⁶ The stiffness is taken to be a function of time in such a way that during laying it reduces first exponentially and then linearly to zero, when laying is complete.

⁷ Infill only affects the foundation coordinates where there are gaps under the pipe, i.e. where the pipe is above the original foundation profile. There are no changes where there has already been some penetration.

t for every step in the analysis, one specifies an increment in arclength on a generalised load-displacement plot of the solution path. The approach adopted not only allows converged solutions up to and beyond the point of loss of stability to be obtained, but moreover it allows the solution to be found even if the buckle forms at an unexpected location or if more than one buckle forms.

6. Results

In almost all cases considered, the pipe would first begin to uplift as indicated by loss of contact with the prop imperfection. The temperature at which this occurs is referred to as the incipient uplift temperature. However a further increase in the temperature of the line is still possible without loss of stability. Then a limit point instability is encountered, beyond which the pipe “jumps” to a new equilibrium configuration in an upheaved state. This limit point occurs at the upheaval buckling temperature.

Both the incipient uplift temperature and the upheaval buckling temperatures are shown in Figure 5 to Figure 8 for a selection of values of the problem parameters. This includes an examination of the effect of reeling (with perfect straightening) in Figure 5 and Figure 7, and of the effect of imperfect straightening of a reeled pipe in Figure 6 and Figure 8.

From Figure 5 it is clear that the infill conditions have much more of an effect on the upheaval buckling temperature than does reeling of the line. Also, for sufficiently high amounts of cover (from 1.5 metres for the case of no infill to 2 metres for the case of infill before covering), reeling results in higher upheaval buckling temperatures. A possible explanation for this is that the loss in flexural resistance is less important for higher amounts of cover, since then one relies more on the cover resistance than on the flexural resistance of the pipe to resist upheaval buckling. On the other hand the loss of the axial driving force due to reeling is independent of the amount of cover. The loss of axial driving force in a fully constrained (and straight) line is shown in Figure 9. Clearly the virgin pipe remains elastic up to temperatures over 160°C. For reeled pipe however, yielding begins much earlier due to the residual stresses and the Baushinger effect. Indeed the application of the pressure alone already causes some yielding, so that even before any temperature changes are applied, the axial force in the reeled line is only about 80% of that in the virgin line. Further yielding occurs in the reeled line as the temperature is increased.

The benefits of soil infill under the pipe are clearly demonstrated by the upheaval buckling temperatures in Figure 5 and Figure 6. For all cases the upheaval buckling temperatures plotted there are higher when infill is present. However for the incipient uplift temperatures of Figure 7 and Figure 8, the situation is different: infill can actually result in a lower incipient uplift temperature, especially for lower amounts of cover and pipe with initial OOS. This occurs because the upward forces the infill exerts upon the pipe can promote earlier incipient uplift at the prop. However, with a small amount of uplift at the prop this effect disappears so that in regard to loss of stability (upheaval buckling) infill has a beneficial effect for all cases considered.

7. Accuracy of Simplified Methods

In this section the finite element results presented are compared to those from simplified methods for sharp props with or without infill after laying.

7.1. Prop without infill

For a sharp prop on a flat seabed (or trench bottom) and no infill, Hobbs [8] derived the following expressions for the required uplift resistance w and the maximum bending moment M_{\max} using elastic beam theory:

$$w = 0.06 \frac{\Delta P^2}{EI}, \quad M_{\max} = 0.36 P \Delta \quad (1a,b)$$

where

Δ = height of prop imperfection

P = effective axial driving force

EI = flexural rigidity of pipe

However, Eq. 1 is not recommended for design, because it is based on a uniformly distributed uplift resistance force, whereas finite element analyses indicate that the maximum uplift resistance force is only developed near the prop. In reality the length of pipe that is held up by the prop imperfection decreases with increasing axial load, so that much of the buckled portion of the pipe is moving downward rather than upwards as the temperature is increased. To assume that uplift resistance acts where the pipe is moving downward is not realistic.

An alternative method to calculate the required uplift resistance focuses on the inflection points to each side of the prop imperfection, where the curvature changes from hogging to sagging. The inflection points have been found to play an important role by Richards [9]. Building on this approach, the following assumptions are adopted herein to derive the required upheaval resistance:

- 1) The elevation of the inflection point remains constant during thermal loading.
- 2) At upheaval buckling, the pipe profile is sinusoidal between inflection points.
- 3) The distribution of uplift resistance force is also sinusoidal, varying from zero at the inflection points to a maximum at the prop.
- 4) The worst possible location of the inflection point along the length of the pipe is assumed.

In this manner a required uplift resistance force over the prop of

$$w = 0.10 \frac{\Delta P^2}{EI} \quad (2)$$

is calculated. The same result is obtained from an analytical solution similar to that of Hobbs, but assuming that the constant uplift resistance force acts only over the 30% of the uplifted portion of the pipe next to the prop, and the vertical force over the remaining 70% is zero.

A comparison of the analytical results from Eq. 2 with those from the finite element simulation is shown in Figure 10. For this comparison, w is taken to be the required uplift resistance at the prop imperfection⁸. For lower temperatures, Eq. 2 is seen to provide a conservative estimate of the required cover. At higher temperatures, however, Eq. 2 underestimates the cover

⁸ This is relevant because the amount of cover material on the pipe is less at the prop than at other locations along the pipe.

requirement. This might be expected, because Eq. 2 is based on linearly elastic pipe behaviour, and at higher temperatures some yielding of the pipe occurs.

To verify the range of validity of Eq. 2, the stresses due to the bending moment of Eq. 1 are combined with those due to axial load and internal pressure to obtain a maximum Von Mises equivalent stress. The point at which this maximum equivalent stress reaches the actual yield stress of 508 MPa is shown in Figure 10 by a solid black triangle identified as the “yield point”.⁹ The assumption of linear elastic behaviour breaks down at temperatures and cover heights beyond this yield point. Throughout the region below the yield point Eq. 2 is seen to provide a reasonable and conservative estimate of the cover requirement.

7.2. Prop with infill before covering

For the case of infill before covering, the foundation imperfection is not sharp, but rather has a wavelength that is determined from the geometry of the pipe as it is laid over the prop imperfection. Assuming the axial forces before covering (due to lay tension) are negligible and using elastic beam theory, this wavelength (from inflection point to inflection point) is found to be

$$L = \left[\frac{35 EI H}{w_p} \right]^{1/4} \quad (3)$$

where

$H = 11 \Delta / 27$ is the difference in elevation from inflection point to the prop,

w_p = submerged weight of flooded pipe,

and the other symbols are as defined for Eq. 1. To derive the required uplift resistance, the same assumptions regarding the sinusoidal pipe profile and distribution of uplift resistance between inflection points are made, except that, instead of assuming the worst possible case for the wavelength between inflection points, the wavelength is obtained from Eq. 3. That is it is assumed that the wavelength remains unchanged during application of the thermal and pressure loads. On this basis the required uplift resistance is found to be:

$$w = \Phi_q \frac{H P^2}{EI} \quad (4)$$

where

$$\Phi_q = \left[\frac{\pi}{\Phi_L} \right]^2 - \left[\frac{\pi}{\Phi_L} \right]^4, \quad \Phi_L = L \sqrt{\frac{P}{EI}} \quad (5a,b)$$

Eq. 4 is intended to be used for buckling wavelengths $\Phi_L \geq 4.44$ (in which case w is a decreasing function of Φ_L). For shorter wavelengths (i.e. $\Phi_L < 4.44$), the uplift resistance should be calculated using a critical buckling wavelength $\Phi_L = 4.44$. For this latter case, the solution is the same as that provided by Eq. 1.

⁹ The actual yield stress rather than the somewhat lower minimum specified yield stress of 448MPa is used here because the intent is to compare the results from the simple analytical formulae to the finite element results, and the latter are also based on actual material properties (given in Figure 2) rather than minimum specified values.

The results of this analytical model are compared in Figure 11 to those from the finite element calculations. To establish the “yield point” of Figure 11 the bending moment is calculated from¹⁰

$$M = 13.1 EI H / L^2 \quad (6)$$

Again there is reasonable agreement between the finite element and simplified analytical results below the “yield point”, although in this case the simplified analytical approach is not always conservative.

An alternative even simpler analytical approach gives rise to the “as laid curvature” result in Figure 11. For this, the required uplift resistance is simply taken to be the as laid curvature of the pipe at the prop multiplied by the effective axial force. This results in

$$w = 13.1 PH / L^2 \quad (7)$$

For pipes that remain elastic, this is seen to give a conservative result because it does not account for the bending resistance of the pipe.

7.3. Updated Design Curve

The above simplified analytical results for the required cover resistance can be expressed in terms of a design curve, which provides the dimensionless required uplift resistance Φ_q as a function of the dimensionless wavelength of the imperfection Φ_L . This design curve is shown in Figure 12 as the “new curve”, together with a number of points representing the results of finite element analyses, and the design curve in [10] which is labelled as the “old curve”. It is clear that the new curve (based on inflection points) provides a better basis for design, since the old curve may be unconservative for short wavelengths of the foundation imperfection. The use of inflection points is not new. Richards [9] also used them. However here the use of inflection points goes further by using the concept used to derive simple formulae for the required uplift resistance.

¹⁰ The highest bending moment is given here, and it occurs as a result of the as-laid curvature before application of the temperature and pressure induced axial loads. The bending moment associated with the sinusoidal pipe profile and uplift resistance force is about 30% smaller.

8. Conclusions

Reeling significantly alters the moment-curvature relation for a pipe, mainly due to residual stresses induced and the Baushinger effect. More specifically there is a decrease in flexural resistance of the pipe, especially for bending in the spooling direction (i.e. for bending in the same direction the pipe is bent when spooled onto the reel). Whereas this decrease in effective bending stiffness has a detrimental effect on upheaval buckling, the residual stresses and Baushinger effect also have a compensatory effect in that they reduce the axial force that develops the line. Indeed the reeled pipe considered already starts to yield under the internal pressure alone. It will also bend under internal pressure alone with no bending moment applied. For the example problem considered, the effective axial force in the reeled pipe under pressure alone is about 20% lower than for the corresponding virgin pipe. The difference increases to 30% at 170°C. In view of the compensatory effects of flexural and axial plastic deformations, the net effect of residual stresses and the Baushinger effect is small, and this effect may be beneficial or detrimental, depending on the conditions considered.

It is conceivable that with time elapsed after reeling of the pipe the residual stresses and the Baushinger effect may diminish as the material “heals”. If that happens, their net effect should be even less than that predicted by these analyses.

Reeling-induced inherent pipe out-of-straightness remains a concern. Especially the combination of assuming infill of gaps under the pipe with material capable of resisting downward motion, and no inherent pipe out-of-straightness, can lead to unconservative design. Furthermore, whereas out-of-straightness can be detected by an on-bottom survey of the pipe, such a survey cannot distinguish between out-of-straightness that is inherent to the pipe, and that which arises due to the foundation profile. Of these two types the inherent pipe out-of-straightness is worse.

The results in this paper highlight the importance of infilling under the pipe. If gaps or weak material exists under the pipe the profile will tend to change for the worse under the action of the thermal loads. As a result the wavelength (from inflection point to inflection point) decreases and the upheaval driving curvature increases. Indeed for the case of a prop with no infill, the finite element (FE) results are well matched by simple analytical formulae based on assuming the worst possible wavelength. With infill on the other hand, by assuming that the wavelength remains unchanged during thermal loading, the FE solution and the analytical model are in good agreement. With or without infill, the analytical model relies on the assumptions that the inflection points remain at the same elevation during loading, and the uplift resistance force varies sinusoidally from zero at the inflection point to a maximum value at the prop.

Given these concerns on imperfections and infill, evidence of achieving minimal pipe out-of-straightness and full sea-bed contact should be provided, or the less favourable case should be assumed in design. Preferably inherent pipe out-of-straightness should be expressed in terms of curvature or the corresponding bending strain, rather than deviation from a straight line over a limited length of pipe.

9. Acknowledgements

The authors are grateful to John Mossman of Shell UK Exploration and Production, who sponsored this work in 1997-98, for his encouragement to publish the findings. A proprietary routine for the Dafalias material model was provided by Professor Stelios Kyriakides from the University of Texas at Austin.

This report also includes revisions as a result of comments by anonymous external reviewers for the Journal of Offshore Mechanics and Arctic Engineering (JOMAE) after the presentation at OMAE 1998. (Although the paper had been accepted, it was not resubmitted to JOMAE, because other priorities had not allowed the required revisions to be completed on time).

References

- [1] Dafalias, Y.F. and Popov, E.P. (1976), "Plastic Internal Variable Formalism of Cyclic Plasticity", *Journal of Applied Mechanics*, December, pp. 645-651.
- [2] Witlox, H.W.M. (1995), "Modelling of Upheaval Buckling of Buried / Trenched Pipelines. Part I: UPBUCK2 Theory", KSEPL External Report, RKER.94.069, November 1995
- [3] Witlox, H.W.M. (1995), "Modelling of Upheaval Buckling of Buried / Trenched Pipelines. Part II: UPBUCK2 User Manual", KSEPL External Report, RKER.94.070, November 1995.
- [4] Hassan, T. and Kyriakides, S. (1992), "Ratcheting in Cyclic Plasticity, Part I: Uniaxial Behaviour", *International Journal of Plasticity*, Vol. 8, pp. 91-116
- [5] Hassan, T., Corona, E. and Kyriakides, S. (1992), "Ratcheting in Cyclic Plasticity, Part II: Multiaxial Behaviour", *International Journal of Plasticity*, Vol. 8, pp. 117-146
- [6] Riks, E. (1979), "Incremental Approach to the Solution of Snapping and Buckling Problems", *Int. J. Solids and Structures*, Vol. 15, pp. 524-551
- [7] Riks, E. and Rankin, C.C. (1987), "Bordered Equations in Continuation Methods: An improved Solution Technique", NLR MP 87057U, National Aerospace Laboratory, The Netherlands
- [8] Hobbs, R. (1984), "In-Service Buckling of Heated Pipelines", *J. Transportation Engineering*, Vol. 110, No. 2, pp. 175-189, March 1984
- [9] Richards, D.M. (1996), "Cover Design for Short Hot Pipelines", OPT 1996
- [10] Palmer, A.C., Ellinas, C.P., Richards, D.M. and Guijt, J., (1990), "Design of Submarine Pipelines Against Upheaval Buckling, Proceedings, 22nd Offshore Technology Conference, Houston, Vol. 2, pp. 551-560, Paper No. OTC 6335

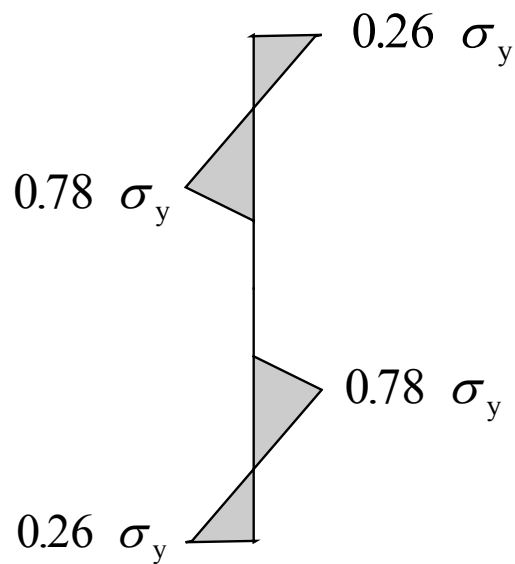


Figure 1: Distribution of axial residual stresses in a pipe reeled to a bending strain of 10 times the yield strain, based on beam theory for elastic-perfectly plastic material behaviour.

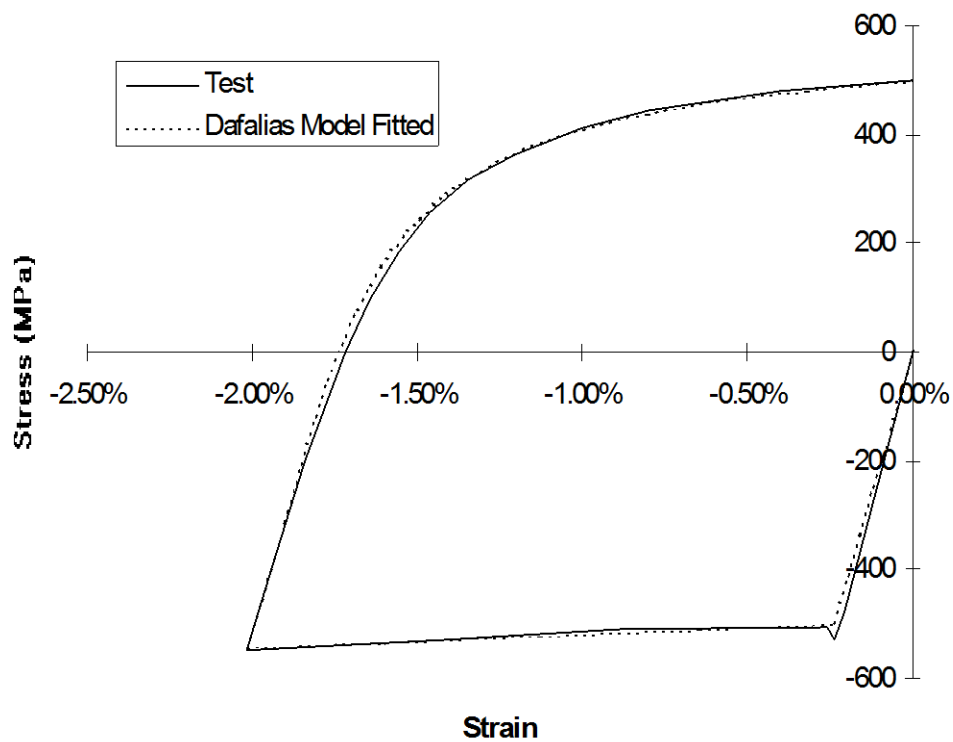


Figure 2: Typical cyclic stress-strain relation from a seamless grade X65 carbon steel pipe. Results are from a coupon test involving loading in the axial direction of the pipe at room temperature. Parameters for Dafalias model [1] fit shown inside figure. (These are the material parameters used for the analyses).

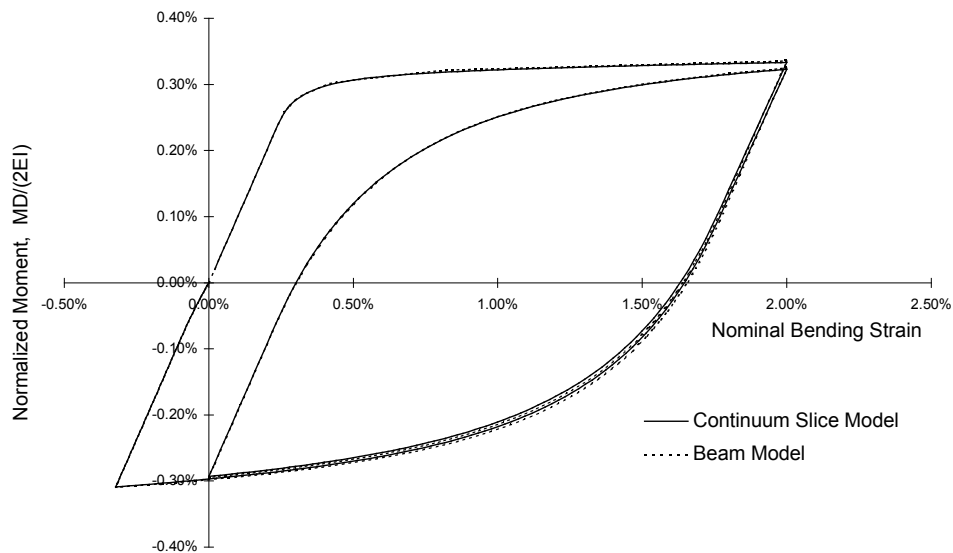


Figure 3: Moment-curvature relationship during reeling for a grade X65 carbon steel pipe with stress-strain behaviour shown in Figure 2 and an outer diameter to thickness ratio of $D/t=20$. [Beam model results do not include ovalisation and are independent of D/t .]

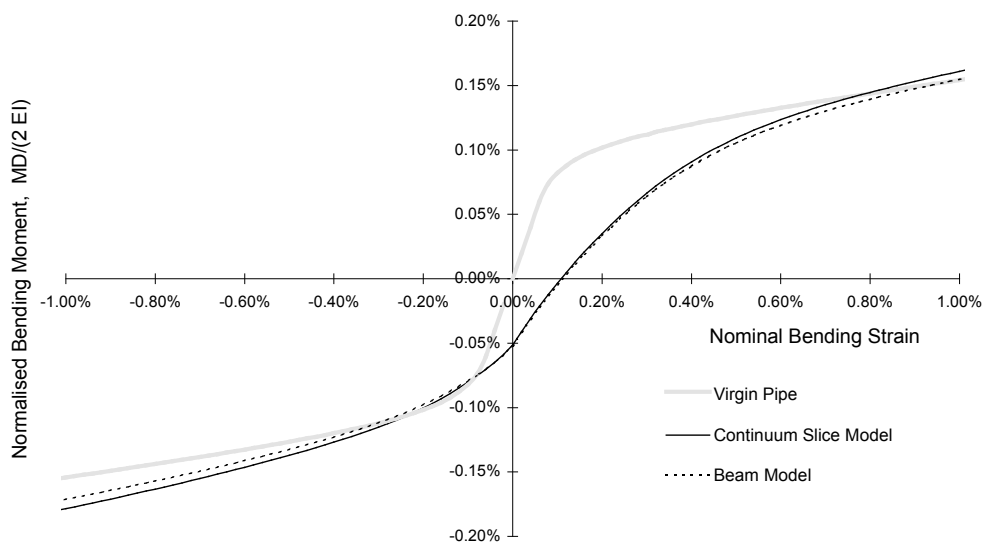


Figure 4: Moment-curvature relationship for an as-laid grade X65 carbon steel pipe with stress-strain behaviour shown in Figure 2 and $D/t=20$. [After reeling the pipe is kept straight while being subjected to internal pressure generating a hoop stress of 72% of the specified minimum yield stress (SMYS), and an axial load equivalent to that which would develop in an axially constrained elastic pipe under internal pressure plus a temperature rise of 1000C. The bending deformations are then applied under constant pressure and axial load].

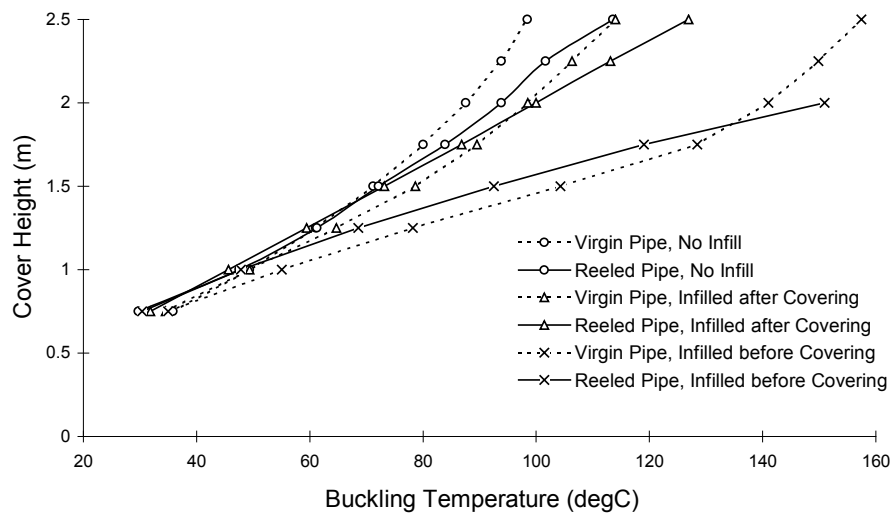


Figure 5: Comparison of upheaval buckling temperatures for reeled pipes (continuous lines) to those for virgin pipe (dotted lines) under various conditions. [ID=200mm, $D/t=15$, Prop Height = 0.3m, grade X65 carbon steel as in Figure 2, No residual curvatures].

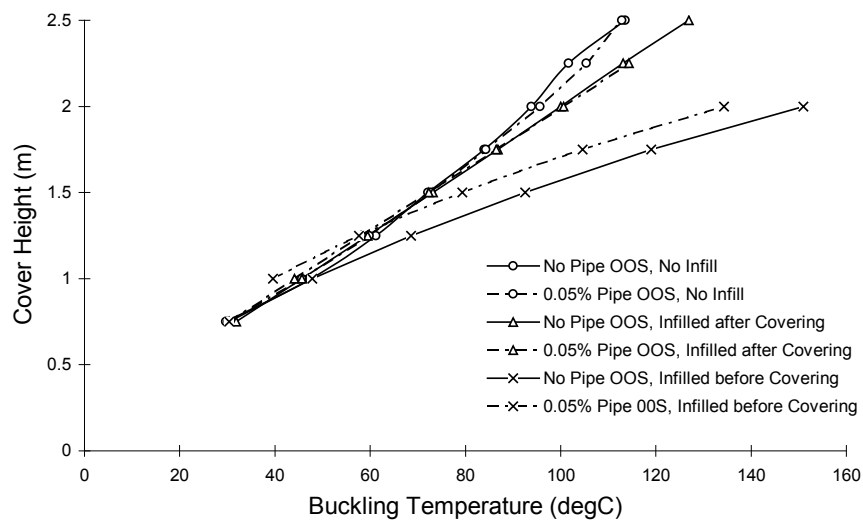


Figure 6: Effect of residual curvature on the upheaval buckling temperature of reeled pipe. The residual curvature corresponds to a bending strain of 0.05% (convex upwards), and is present over a length of 5m to each side of the prop imperfection. [ID=200mm, $OD/t=15$, Prop Height=0.3m, X65 carbon steel as in Figure 2, Reeled Pipe for all cases].

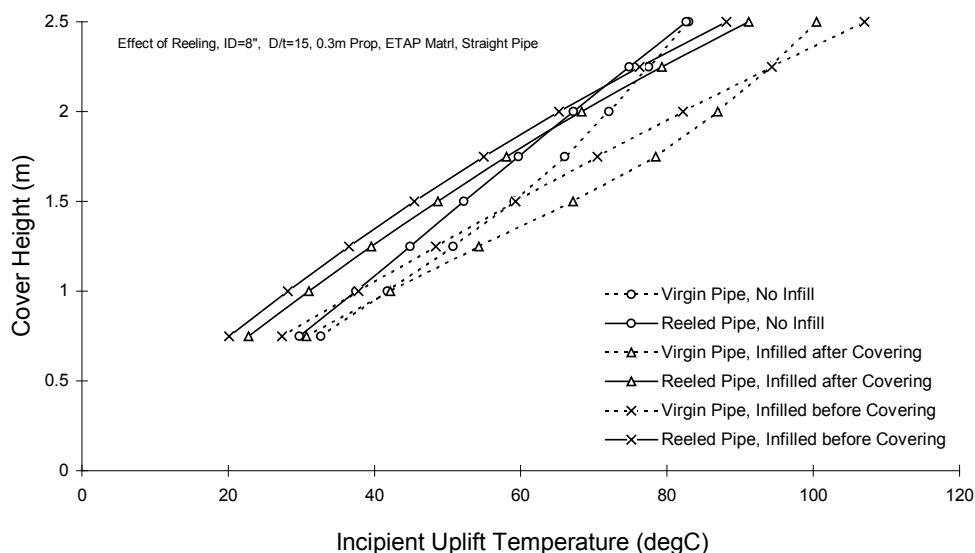


Figure 7: Comparison of incipient uplift temperatures for reeled pipes (continuous line) to those for virgin pipe (dotted lines) under various conditions. The incipient uplift temperature is defined as the temperature at which the pipe first loses contact from the prop foundation imperfection. [ID=200mm, OD/t=15, Prop Height = 0.3m, X65 carbon steel as in Figure 2, No residual curvatures].

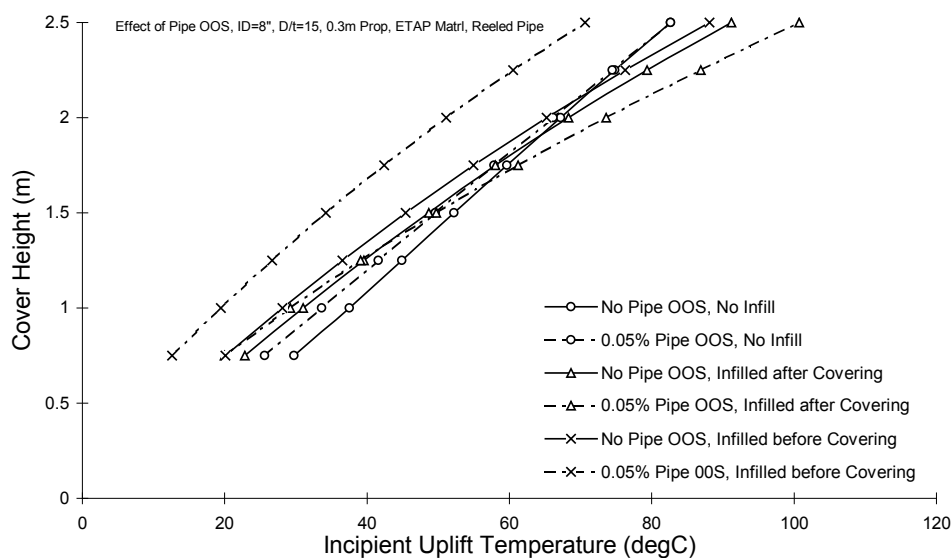


Figure 8: Effect of residual curvature on the incipient uplift temperature of reeled pipe. The residual curvature corresponds to a bending strain of 0.05% (convex upwards), and is present over a length of 5m to each side of the prop imperfection. [ID=200mm, OD/t=15, Prop Height=0.3m, X65 carbon steel as in Figure 2, Reeled Pipe for all cases].

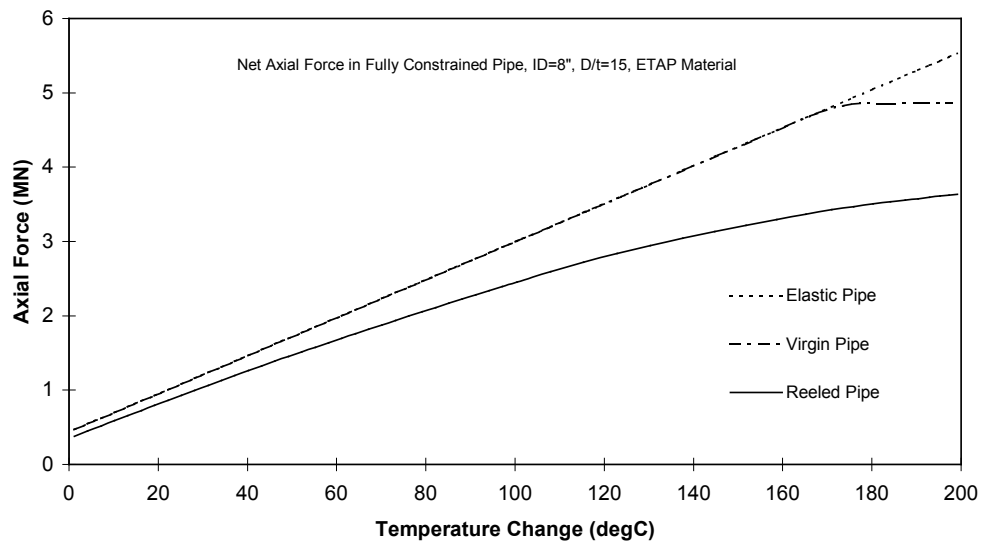


Figure 9: Effect of reeling on effective net axial force developed in a fully constrained line

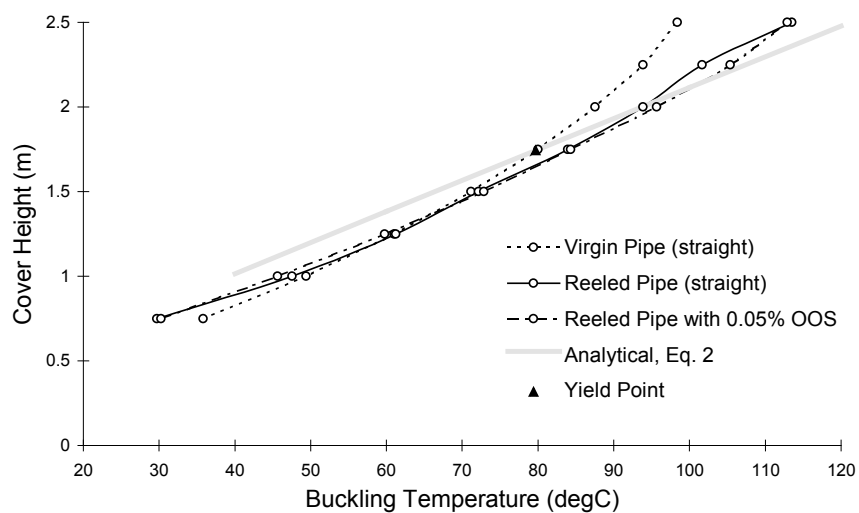


Figure 10: Comparison of upheaval buckling temperatures for case of no infill. [ID=200mm, OD/t=15, Prop Height=0.3, X65 Carbon steel as in Figure 2].

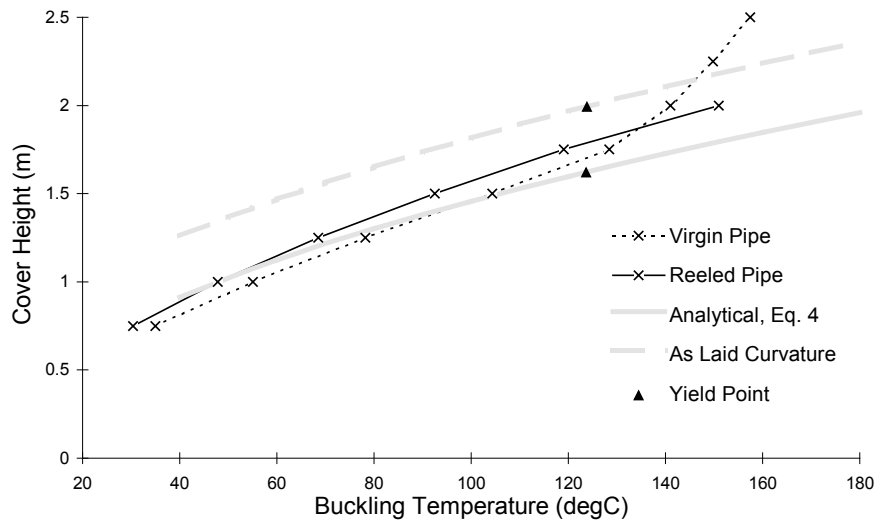


Figure 11: Comparison of upheaval buckling temperatures for case when any gaps under the pipe are filled in with soil before covering. [ID=200mm, OD/t=15, Prop Height=0.3, X65 Carbon steel as in Figure 2].

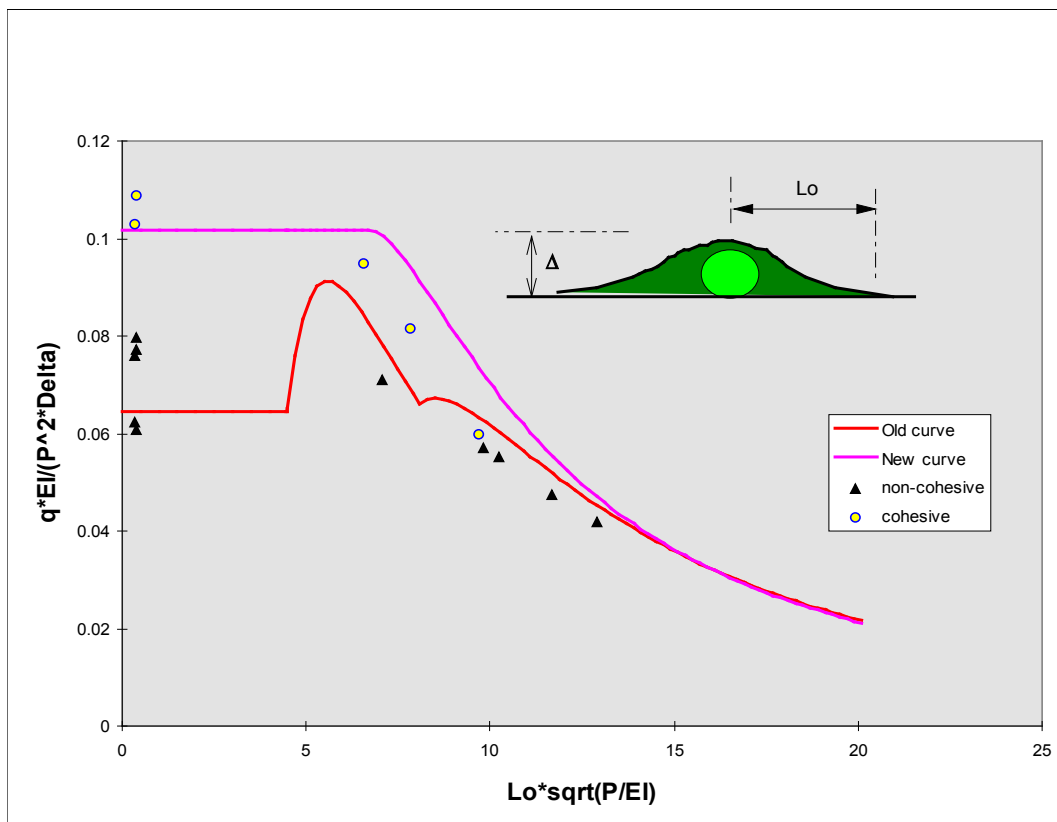


Figure 12: Updated design curve for the dimensionless required uplift resistance Φ_q (Eq. 4) as a function of the dimensionless wavelength of the imperfection Φ_L (Eq. 5b), and comparison with results from finite element analyses.

Bibliographic information

Classification	Unrestricted
Report Number	SR.12.12579
Title	Upheaval buckling of reeled flowlines
Author(s)	R. Peek (GSNL-PTE/EPFA) G. Stewart (Lloyd's Register of Shipping, Aberdeen)
Keywords	pipeline, reeling, upheaval buckling, OOS, offshore, high-temperature, HPHT
Date of Issue	August 2012
US Export Control	Public Domain
WBSE Code	ZZPT/015338/011003
Reviewed by	F. Kopp (PTP/ADS)
Approved by	S. Simons (PTE/EPFA)
Sponsoring Company / Customer	SGSI
Issuing Company	Shell Global Solutions International B.V. P.O. Box 60 2280 AB Rijswijk The Netherlands

Report distribution

Electronic distribution (PDF)

Name, Company, Ref. Ind.

PDF

PT Information Services, PTT/TIKE, PT-Information-Services@Shell.com

Word + PDF

Kopp, Frans SIEP-PTP/ADS

PDF

Guijt, Wim GSNL-PTE/EPFA

PDF

Simons, Servie JM GSNL-PTE/EPFA

PDF

Yun, Heedo SIEP-PTP/ADS

PDF

Peek, Ralf GSNL-PTE/EPFA

PDF

The copyright of this document is vested in Shell Global Solutions International, B.V. The Hague, The Netherlands. All rights reserved.

Neither the whole nor any part of this document may be reproduced, stored in any retrieval system or transmitted in any form or by any means (electronic, mechanical, reprographic, recording or otherwise) without the prior written consent of the copyright owner. Shell Global Solutions is a trading style used by a network of technology companies of the Shell Group.